

Adaptive generalized multiscale finite element methods for H(curl)-elliptic problems with heterogeneous coefficients

Eric T. Chung* and Yanbo Li†

July 11, 2018

Abstract

In this paper, we construct an adaptive multiscale method for solving H(curl)-elliptic problems in highly heterogeneous media. Our method is based on the generalized multiscale finite element method. We will first construct a suitable snapshot space, and a dimensional reduction procedure to identify important modes of the solution. We next develop and analyze an a posteriori error indicator, and the corresponding adaptive algorithm. In addition, we will construct a coupled offline-online adaptive algorithm, which provides an adaptive strategy to the selection of offline and online basis functions. Our theory shows that the convergence is robust with respect to the heterogeneities and contrast of the media. We present several numerical results to illustrate the performance of our method.

1 Introduction

Many practical problems are modeled by partial differential equations with highly heterogeneous coefficients. Classical numerical methods for solving these problems typically require very fine computational meshes, and are therefore very expensive to use. In order to solve these problems efficiently, one needs some types of model reduction, which is typically based on upscaling techniques or multiscale methods. In upscaling methods, the heterogeneous coefficient is carefully replaced by an effective medium [14, 29, 20, 23] so that the system can be solved on a much coarser grid. In multiscale methods, such as those in [2, 3, 19, 16, 17, 18, 22, 8, 4, 13, 21, 1, 26], one attempts to represent the solution by some multiscale basis functions. These basis functions are constructed carefully and are usually based on some local cell problems. The purpose is to capture the fine scale properties of the true solution by using a few multiscale basis functions, with the aim of reducing computational costs.

In this paper, we consider the H(curl)-elliptic problem with highly heterogeneous coefficients. Our aim is to construct a multiscale method for solving this problem. We will consider the generalized multiscale finite element method (GMsFEM) [15, 5]. GMsFEM is a generalization of the classical multiscale finite element method [25] in the way that multiple basis functions are used for

*Department of Mathematics, The Chinese University of Hong Kong (CUHK), Hong Kong SAR. Email: tschung@math.cuhk.edu.hk. The research of Eric Chung is supported by Hong Kong RGC General Research Fund (Project 14317516) and CUHK Direct Grant for Research 2016-17.

†Department of Mathematics, Texas A&M University, College Station, TX 77843. Email: lyb@tamu.edu.

each coarse region. We will consider three important components of the GMsFEM in this paper. The first one is basis functions construction. This is a process in the offline stage. To find the basis functions, we will construct a set of snapshot functions for each local coarse region. The snapshot functions are solutions of local cell problems with some suitable boundary conditions. To obtain the offline basis functions, we perform a dimension reduction procedure by using a suitable spectral problem, designed carefully based on analysis. These basis functions are then used in a coarse scale conforming finite element formulation to solve the problem. The second component is offline adaptivity [12]. In order to determine the number of offline basis functions to be used for each coarse region, we will develop a local error indicator based on an a posteriori error analysis. Using the proposed error indicator, we are able to determine the number of basis functions in an adaptive way. In addition, we prove the convergence of this approach, and show that the convergence rate is independent of the heterogeneities of the coefficients. The last component is online adaptivity [10]. The goal of online basis functions is to capture some components, such as global feature, of the solution that are not representable by offline basis functions. To compute online basis functions, we solve local cell problems by using local residual of the solution. Moreover, we can do this in an adaptive way, so that online basis functions are only added in regions with larger errors. We prove the convergence of the online adaptive method and show that the convergence rate is independent of the coefficients. We also show that a sufficient number of offline basis functions is needed in order to obtain a rapid convergence rate of the online adaptive method. We remark that there are also related methods developed for the discontinuous Galerkin formulation in [7] and [9]. We also remark that a method based on HMM is developed in [24].

To illustrate the performance of our GMsFEM, we present some numerical results focusing on the convergence properties of the method. We will first show that the method is robust with respect to the contrast and heterogeneities of the coefficients. Next, we illustrate the advantage of using offline adaptivity by comparing the convergence behaviour with uniform basis enrichment, and show that the offline adaptive method is able to capture the solution more effectively. Finally, we construct a coupled offline-online adaptive method. It is known that the first few offline basis functions correspond to the dominant components of the solution, and the rest of the offline basis functions contribute the solution in a less crucial way. So, one needs to switch to the use of online basis functions once sufficient number of offline basis functions are used. Our offline-online adaptive method allows this to be done automatically. By using a suitable error indicator and a suitable tolerance parameter, we show that the offline-online adaptive method performs very well and give a practical solver for realistic applications.

The rest of the paper is organized as follows. In the next section, we briefly introduce the basic idea of the GMsFEM. In Section 3, we will present both the offline and the online adaptive methods, and in Section 4, we will analyze these methods. In Section 5, numerical results are presented to illustrate the performance of the adaptive methods. Finally, the paper ends with a conclusion.

2 The GMsFEM

In this section, we will give the construction of our GMsFEM for $H(\text{curl})$ -elliptic problem. First, we present some basic notations and the coarse grid formulation in Section 2.1. Then, we present the constructions of the multiscale snapshot functions, basis functions and the multiscale scheme in Section 2.2. We will mainly present our ideas in the two-dimensional settings. The extension to the three-dimensional case is straightforward.

2.1 Preliminaries

Let D be a bounded domain in \mathbb{R}^2 with a Lipschitz boundary ∂D with unit tangential vector t . In this paper, we consider the following high-contrast $H(\text{curl})$ -elliptic problem

$$\begin{aligned} \nabla \times (a \nabla \times u) + b u &= f && \text{in } D, \\ u \cdot t &= 0 && \text{on } \partial D, \end{aligned} \quad (1)$$

where $a \geq 1$ is a heterogeneous field with high contrast, $b > 0$ is a bounded heterogeneous field and f is a given divergence-free source.

To describe the general solution framework for the model problem (1), we first introduce the notion of fine and coarse grids. Let \mathcal{T}^h be a partition of the domain D into fine finite elements. Here $h > 0$ is the fine mesh size. The coarse partition, \mathcal{T}^H of the domain D , is formed such that each element in \mathcal{T}^H is a connected union of fine-grid blocks. More precisely, $\forall K_j \in \mathcal{T}^H$, $K_j = \cup_{F \in I_j} F$ for some $I_j \subset \mathcal{T}^h$. The quantity $H > 0$ is the coarse mesh size. We will consider rectangular coarse elements and the methodology can be used with general coarse elements. An illustration of the mesh notations is shown in Figure 1(Left).

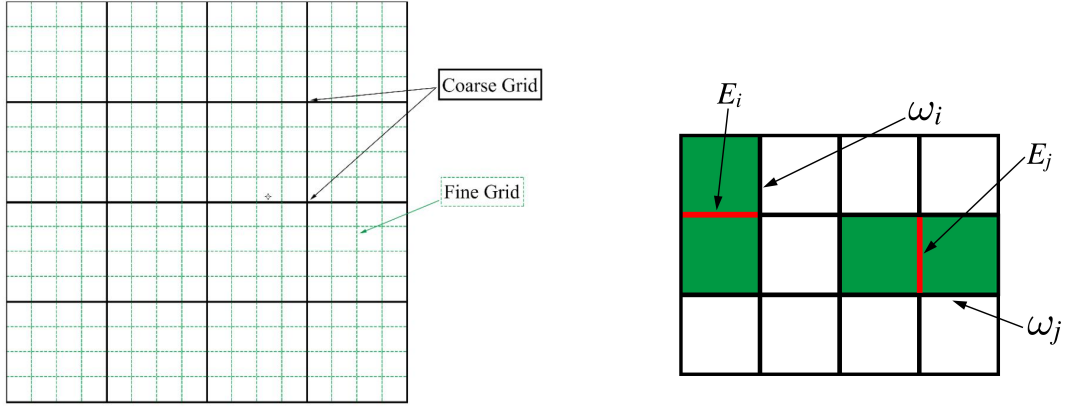


Figure 1: Left: an illustration of fine and coarse grids. Right: an illustration of a coarse neighborhood and a coarse element.

Next, we define the finite element space V_h as the set of the lowest order curl conforming elements of Nédélec with respect to the fine mesh \mathcal{T}^h , and define $V_h^0 = \{v \in V_h \mid v \cdot t = 0 \text{ on } \partial D\}$. The fine-scale solution $u_h \in V_h$ is obtained by solving the following variational problem

$$\int_D \left(a (\nabla \times u_h) (\nabla \times v) + b u_h \cdot v \right) = \int_D f \cdot v \quad \forall v \in V_h^0. \quad (2)$$

The solution u_h is our reference solution. The convergence property of this method is well-known (see for example [28]).

Finally, for any subdomain $\Omega \subset D$, and $v \in V_h$, we define the norms $\|v\|_{L^2(b;\Omega)}$ and $\|v\|_{H(\text{curl})(a,b;\Omega)}$ as

$$\|v\|_{L^2(b;\Omega)}^2 = \int_{\Omega} b |v|^2$$

and

$$\|v\|_{H(\text{curl})(a,b;\Omega)}^2 = \int_{\Omega} a |\nabla \times v|^2 + b |v|^2.$$

2.2 Construction of multiscale basis functions

In this section, we will give the constructions of our GMSFEM. In Section 2.2.1, we will present the construction of the snapshot space. To do so, we will locally solve the $H(\text{curl})$ -elliptic problem on coarse neighborhoods with suitable boundary conditions. This process will provide a set of functions which are able to span the fine-scale solution with high accuracy. Next, in Section 2.2.3, we will present the construction of our multiscale basis functions. The construction is based on the design of a suitable local spectral problem which can identify important modes in the snapshot space. Finally, we present our multiscale method.

2.2.1 Snapshot Space

We denote the set of all edges of the coarse grid as \mathcal{E}^H , and let N_e be the total number of interior edges of the coarse grid. We define the coarse grid neighborhood ω_i of an edge $E_i \in \mathcal{E}^H$ as

$$\omega_i = \bigcup \{K \in \mathcal{T}^H : E_i \in \partial K\}$$

which is the union of all coarse grid blocks having the edge E_i . This concept is illustrated in Figure 1 (Right).

In each ω_i corresponding to an interior coarse edge E_i , we will solve the following local problem

$$\begin{aligned} \nabla \times (a \nabla \times \psi_j^{(i)}) + b \psi_j^{(i)} &= 0, & \text{in each element } K \subset \omega_i, \\ \psi_j^{(i)} \cdot t &= 0, & \text{on } \partial\omega_i, \\ \psi_j^{(i)} \cdot t &= \delta_j^{(i)}, & \text{on } \partial E_i. \end{aligned} \quad (3)$$

In the above problem, we write $E_i = \bigcup_{j=1}^{J_i} e_j$, where e_j 's are the fine grid edges contained in E_i , and we define

$$\delta_j^{(i)} = \begin{cases} 1, & \text{on } e_j, \\ 0, & \text{on } E_i \setminus e_j. \end{cases}$$

The set of solutions to problem (3) is the local snapshot basis $\beta_{\text{snap}}^{(i)}$. The local snapshot space $V_{\text{snap}}^{(i)}$ corresponding to the coarse neighborhood ω_i is defined as the span of all the above functions, that is, $V_{\text{snap}}^{(i)} = \text{span}(\beta_{\text{snap}}^{(i)})$. The global snapshot space, or simply the snapshot space, is defined as $V_{\text{snap}} = \bigoplus_{i=1}^{N_e} V_{\text{snap}}^{(i)}$. After we construct V_{snap} , we can solve snapshot solution $u_{\text{snap}} \in V_{\text{snap}}$ by solving

$$\int_D \left(a (\nabla \times u_{\text{snap}})(\nabla \times v) + b u_{\text{snap}} \cdot v \right) = \int_D f \cdot v, \quad \forall v \in V_{\text{snap}}. \quad (4)$$

2.2.2 Snapshot error

In this section, we will show that the difference between the fine scale solution u_h and the snapshot solution u_{snap} is $O(H)$.

Theorem 1. Let $u_h \in V_h$ be the solution of (2) and let $u_{\text{snap}} \in V_{\text{snap}}$ be the solution of (4). Then we have

$$\|u_h - u_{\text{snap}}\|_{H(\text{curl})(a,b;D)} \leq CH \|f\|_{L^2(D)},$$

where C is independent of a and b .

Proof. We choose $\widehat{u_{\text{snap}}} \in V_{\text{snap}}$ such that $\widehat{u_{\text{snap}}} \cdot t = u_h \cdot t$ on \mathcal{E}^H . In particular, in each coarse block K , the following equations hold

$$\begin{aligned} \nabla \times (a \nabla \times (u_h - \widehat{u_{\text{snap}}})) + b (u_h - \widehat{u_{\text{snap}}}) &= f, & \text{in } K, \\ (u_h - \widehat{u_{\text{snap}}}) \cdot t &= 0, & \text{on } \partial K. \end{aligned}$$

The corresponding variational problem is

$$\int_K a (\nabla \times (u_h - \widehat{u_{\text{snap}}})) (\nabla \times v) + b (u_h - \widehat{u_{\text{snap}}}) \cdot v = \int_K f \cdot v \quad \forall v \in V_h^0(K), \quad (5)$$

where $V_h^0(K) = \{v \text{ is Nédélec elements in } K \mid v \cdot t = 0 \text{ on } \partial K\}$. Taking $v = u_h - \widehat{u_{\text{snap}}} \in V_h^0(K)$ in the above equation, we have

$$\begin{aligned} \|u_h - \widehat{u_{\text{snap}}}\|_{H(\text{curl})(a,b;K)}^2 &= \int_K f \cdot (u_h - \widehat{u_{\text{snap}}}) \\ &\leq \|f\|_{L^2(K)} \|u_h - \widehat{u_{\text{snap}}}\|_{L^2(K)}. \end{aligned} \quad (6)$$

Moreover, for any $p \in Q_h^0(K)$, where Q_h^0 represents the space of piecewise bilinear functions in fine grid with zero boundary condition, we take $v = \nabla p \in V_h^0(K)$ in (5). Since f is divergence-free, we have

$$\int_K b (u_h - \widehat{u_{\text{snap}}}) \cdot \nabla p = 0.$$

Therefore $u_h - \widehat{u_{\text{snap}}}$ is discrete divergence-free.

By Lemma 7.20 in [27], we have

$$\|u_h - \widehat{u_{\text{snap}}}\|_{L^2(b;K)}^2 \leq c |u_h - \widehat{u_{\text{snap}}}|_{H(\text{curl})(K)}^2 \leq c |u_h - \widehat{u_{\text{snap}}}|_{H(\text{curl})(a;K)}^2,$$

where the semi-norm $|v|_{H(\text{curl})(a;K)}$ is defined as

$$|v|_{H(\text{curl})(a;K)}^2 = \int_K a |\nabla \times v|^2.$$

Note that c is independent of a .

By rescaling, we have

$$\|u_h - \widehat{u_{\text{snap}}}\|_{L^2(b;K)}^2 \leq c' H^2 |u_h - \widehat{u_{\text{snap}}}|_{H(\text{curl})(a;K)}^2.$$

Therefore,

$$\begin{aligned} \|u_h - \widehat{u_{\text{snap}}}\|_{L^2(b;K)}^2 &\leq \frac{c' H^2}{1 + c' H^2} \|u_h - \widehat{u_{\text{snap}}}\|_{H(\text{curl})(a,b;K)}^2 \\ &\leq c' H^2 \|u_h - \widehat{u_{\text{snap}}}\|_{H(\text{curl})(a,b;K)}^2. \end{aligned}$$

Combining with (6), we have

$$\|u_h - \widehat{u_{\text{snap}}}\|_{H(\text{curl})(a,b;K)}^2 \leq c' H^2 \|f\|_{L^2(K)}^2.$$

By Cea's inequality, we have

$$\begin{aligned} \|u_h - u_{\text{snap}}\|_{H(\text{curl})(a,b;K)}^2 &= \inf_{v \in V_{\text{snap}}} \|u_h - v\|_{H(\text{curl})(a,b;K)}^2 \\ &\leq \|u_h - \widehat{u_{\text{snap}}}\|_{H(\text{curl})(a,b;K)}^2 \\ &\leq c' H^2 \|f\|_{L^2(K)}^2 \end{aligned}$$

Therefore,

$$\begin{aligned} \|u_h - u_{\text{snap}}\|_{H(\text{curl})(a,b;D)}^2 &= \sum_K \|u_h - u_{\text{snap}}\|_{H(\text{curl})(a,b;K)}^2 \\ &\leq \sum_K c' H^2 \|f\|_{L^2(K)}^2 \\ &= c' H^2 \|f\|_{L^2(D)}^2. \end{aligned}$$

□

2.2.3 Offline Space

After we obtain the snapshot spaces V_{snap} , we perform a dimension reduction to get a smaller space. Such reduced space is called the offline space. The reduction is achieved by solving a local spectral problem on each coarse grid neighborhood ω_i . The dominant eigenfunctions will be used to form the local basis $\beta_{\text{ms}}^{(i)}$. The local spectral problem, in each ω_i , is to find real number λ and $v \in V_{\text{snap}}^{(i)}$ such that

$$a_i(v, w) = \lambda s_i(v, w), \quad \forall w \in V_{\text{snap}}^{(i)}, \quad (7)$$

where

$$\begin{aligned} a_i(v, w) &= \int_{E_i} b(v \cdot t)(w \cdot t), \\ s_i(v, w) &= \frac{1}{H} \int_{\omega_i} a(\nabla \times v)(\nabla \times w) + b v \cdot w. \end{aligned}$$

The term $1/H$ is added so that a_i and s_i have the same scale. Note that this does not alter the eigenfunctions. After solving the spectral problem in each ω_i , we arrange the eigenfunctions $\phi_j^{(i)}$, in ascending order of the corresponding eigenvalues $\lambda_1^{(i)} \leq \lambda_2^{(i)} \leq \dots \leq \lambda_{j_i}^{(i)}$. We then let $\beta_{\text{ms}}^{(i)}$ be the set of the first l_i eigenfunctions, where l_i be the number of offline basis functions. And define local offline space as $V_{\text{ms}}^{(i)} = \text{span}(\beta_{\text{ms}}^{(i)})$ and global offline space as $V_{\text{ms}} = \bigoplus_{i=1}^{N_e} V_{\text{ms}}^{(i)}$. Finally, the GMsFEM is defined as follows. We find $u_{\text{ms}} \in V_{\text{ms}}$ by solving

$$\int_D \left(a(\nabla \times u_{\text{ms}})(\nabla \times v) + b u_{\text{ms}} \cdot v \right) = \int_D f \cdot v, \quad \forall v \in V_{\text{ms}}. \quad (8)$$

3 Adaptive selection of basis functions

In our GMsFEM (9), one needs to choose the number of basis functions for each coarse neighborhood. An attractive and practical strategy is to do this adaptively. In particular, the number of basis functions is determined by some local residuals, which measure the accuracy of the solution. There are two related concepts, namely offline and online adaptivity. In Section 3.1, we will present the offline adaptivity and in Section 3.2, we will present the online adaptivity.

3.1 Offline adaptive Method

In this section, we will introduce an error indicator on each coarse grid neighborhood. Based on this estimator, we develop an offline adaptive enrichment method to solve equation (1) iteratively by adding offline basis functions supported on some coarse grid neighborhoods in each iteration. We emphasize that all selected basis functions come from the spectral problem (7).

Notice that the offline adaptive method is an iterative process. We use the notation u_{ms}^m to denote the multiscale solution at the m -th iteration. For each ω_i , we define the local residual operator R_i^m as a linear functional on $V_{\text{snap}}^{(i)}$ by

$$R_i^m(v) = \int_{\omega_i} a(\nabla \times u_{\text{ms}}^m)(\nabla \times v) + b u_{\text{ms}}^m \cdot v - f \cdot v, \quad \forall v \in V_{\text{snap}}^{(i)}.$$

We take $(\eta_i^m)^2 = \|R_i^m\|^2 (\lambda_{i+1}^{(i)})^{-1}$, $\eta_i^m \geq 0$ as our error indicator, where

$$\|R_i^m\| = \sup_{v \in V_{\text{snap}}^{(i)}} \frac{|R_i^m(v)|}{\|v\|_{H(\text{curl})(a,b;\omega_i)}}.$$

Offline adaptive method: Fix the number θ and δ_0 with $0 \leq \theta, \delta_0 < 1$.

We start with iteration number $m = 0$. Fix *initial number* of offline basis functions l_i^0 for each ω_i to form the offline space V_{ms}^0 . Then, we go to step 1 below

Step 1: Find the multiscale solution. We solve multiscale solution $u_{\text{ms}}^m \in V_{\text{ms}}^m$ satisfying

$$\int_D a(\nabla \times u_{\text{ms}}^m)(\nabla \times v) + b u_{\text{ms}}^m \cdot v = \int_D f \cdot v \quad \forall v \in V_{\text{ms}}^m. \quad (9)$$

Step 2: Compute the error indicators. For each coarse grid neighborhood ω_i , we compute the local error indicator η_i^m and rearrange the local error indicators in decreasing order $\eta_1^m \geq \eta_2^m \geq \dots \geq \eta_{N_e}^m$.

Step 3: Select the coarse grid neighborhoods where basis enrichment is needed. We take the smallest k , such that

$$\theta \sum_{i=1}^{N_e} (\eta_i^m)^2 \leq \sum_{i=1}^k (\eta_i^m)^2.$$

We will enrich the offline space by adding basis functions which are supported in $\omega_1, \omega_2, \dots, \omega_k$.

Step 4: Add basis functions to the space. For those ω_i 's selected from Step 3, we will take the smallest s_i such that $\frac{\lambda_i^{(i)m+1}}{\lambda_i^{(i)m+s_i+1}} \leq \delta_0$. We then set $l_i^{m+1} = l_i^m + s_i$. And for other ω_i 's, we set $l_i^{m+1} = l_i^m$.

After Step 4, we repeat from Step 1 until the global error indicator $\sum_{i=1}^{Ne} (\eta_i^m)^2$ is small enough or the total number of basis functions reaches certain level. The calculations of all the local error indicators can be costly. However, since the error indicators are independent of each other, the computation can be done in a parallel approach in order to enhance the efficiency.

3.2 Online adaptive Method

Next, we will present another enrichment algorithm which requires the formation of new basis functions based on the solution of the previous enrichment level. We call these functions online basis functions as these basis functions are computed in the online stage of computations. With the addition of the online basis functions, we can get a much faster convergence rate than the offline adaptive method. We emphasize that the basis functions are solved using local residuals, and they are not from the spectral problem (7).

We first define a linear functional which generalizes the residual operator in the offline adaptive method. Given a region $\Omega \subset D$ which is a union of some ω_i 's, we define $V_\Omega = \bigoplus_{\omega_i \subset \Omega} V_{\text{snap}}^{(i)}$. And define the linear operator R_Ω^m on V_Ω , and the norm $\|R_\Omega^m\|$ by

$$R_\Omega^m(v) = \int_{\Omega} a(\nabla \times u_{\text{ms}}^m)(\nabla \times v) + b u_{\text{ms}}^m \cdot v - f \cdot v, \quad \forall v \in V_\Omega,$$

$$\|R_\Omega^m\| = \sup_{v \in V_\Omega} \frac{|R_\Omega^m(v)|}{\|v\|_{H(\text{curl})(a,b;\Omega)}}.$$

Online adaptive method: We start with iteration number $m = 0$. Fix *initial number* of offline basis functions l_i for each ω_i to form the offline space V_{ms}^0 . Then

Step 1: Find the multiscale solution. We solve multiscale solution $u_{\text{ms}}^m \in V_{\text{ms}}^m$ satisfying (9) in Offline Adaptive Method.

Step 2: Select non-overlapping regions. We pick non-overlapping region $\Omega_1^m, \Omega_2^m, \dots, \Omega_{j_m}^m \subset D$ such that each Ω_j^m is a union of some ω_i 's.

Step 3: Solve for online basis functions. For each Ω_j^m , we solve $\phi_j^m \in V_{\Omega_j^m}$ such that

$$R_{\Omega_j^m}^m(v) = \int_{\Omega_j^m} a(\nabla \times \phi_j^m)(\nabla \times v) + b \phi_j^m \cdot v, \quad \forall v \in V_{\Omega_j^m}.$$

Then we set $V_{\text{ms}}^{m+1} = V_{\text{ms}}^m \bigoplus \{\phi_1^m, \phi_2^m, \dots, \phi_{j_m}^m\}$.

Note that: By Riesz Representation Theorem, $\|\phi_j^m\|_{H(\text{curl})(a,b;\Omega)} = \|R_{\Omega_j^m}^m\|$.

After Step 3, we repeat from Step 1 until the global error indicator is small or we have used a certain number of basis functions.

4 Convergence Analysis

In this section, we will present the proofs for the convergence of both the offline and the online adaptive methods. We begin with the following a posteriori error bound for the offline adaptive method.

Theorem 2. *Let $u_{\text{snap}} \in V_{\text{snap}}$ be the solution of (4) and let $u_{\text{ms}} \in V_{\text{ms}}$ be the solution of (9). Then we have*

$$\|u_{\text{snap}} - u_{\text{ms}}\|_{H(\text{curl})(a,b;D)}^2 \leq C_{\text{err}} \sum_{i=1}^{N_e} \|R_i\|^2 (\lambda_{l_i+1}^{(i)})^{-1}$$

where $C_{\text{err}} = \frac{C_V H}{h}$. The value of C_V depends on the polynomial order of the fine grid basis functions in V_{snap} . Here we omit superscript m for brevity of notation.

Proof. We define the global residual operator R as a linear functional on V_{snap} by

$$R(v) = \int_D a (\nabla \times u_{\text{ms}}) (\nabla \times v) + b u_{\text{ms}} \cdot v - f \cdot v, \quad \forall v \in V_{\text{snap}}.$$

Thus we have

$$\begin{aligned} -R(u_{\text{snap}} - u_{\text{ms}}) &= \int_D a (\nabla \times u_{\text{ms}}) (\nabla \times (u_{\text{snap}} - u_{\text{ms}})) + b u_{\text{ms}} \cdot (u_{\text{snap}} - u_{\text{ms}}) \\ &\quad - f \cdot (u_{\text{snap}} - u_{\text{ms}}). \end{aligned} \quad (10)$$

Taking $v = u_{\text{snap}} - u_{\text{ms}}$ in (4), we have

$$0 = \int_D a (\nabla \times u_{\text{snap}}) (\nabla \times (u_{\text{snap}} - u_{\text{ms}})) + b u_{\text{snap}} \cdot (u_{\text{snap}} - u_{\text{ms}}) - f \cdot (u_{\text{snap}} - u_{\text{ms}}). \quad (11)$$

Adding (10) and (11), we have

$$\begin{aligned} -R(u_{\text{snap}} - u_{\text{ms}}) &= \int_D a |\nabla \times (u_{\text{snap}} - u_{\text{ms}})|^2 + b |u_{\text{snap}} - u_{\text{ms}}|^2 \\ &= \|u_{\text{snap}} - u_{\text{ms}}\|_{H(\text{curl})(a,b;D)}^2. \end{aligned}$$

Next, we decompose $u_{\text{snap}} - u_{\text{ms}}$ as the sum of functions from $V_{\text{snap}}^{(i)}$'s, that is, we write $u_{\text{snap}} - u_{\text{ms}} = \sum_{i=1}^{N_e} v^{(i)}$ where $v^{(i)} \in V_{\text{snap}}^{(i)}$. And each $v^{(i)}$ is a sum of two functions which are from $V_{\text{ms}}^{(i)}$ and $V_{\text{snap}}^{(i)} \setminus V_{\text{ms}}^{(i)}$, respectively. We denote the function from $V_{\text{snap}}^{(i)} \setminus V_{\text{ms}}^{(i)}$ by $v_r^{(i)}$.

By the definition of R_i and (9), we know $R_i(v) = 0$ for all $v \in V_{\text{ms}}^{(i)} \subset V_{\text{ms}}$. Therefore, $R_i(v^{(i)}) = R_i(v_r^{(i)})$. So, we have

$$R(u_{\text{snap}} - u_{\text{ms}}) = \sum_{i=1}^{N_e} R(v^{(i)}) = \sum_{i=1}^{N_e} R_i(v^{(i)}) = \sum_{i=1}^{N_e} R_i(v_r^{(i)}).$$

Using the definition of the spectral problems, we get

$$|-R(u_{\text{snap}} - u_{\text{ms}})| = \left| \sum_{i=1}^{N_e} R_i(v_r^{(i)}) \right| \leq \sum_{i=1}^{N_e} |R_i(v^{(i)})| \leq \sum_{i=1}^{N_e} \|R_i\| \left(s_i(v_r^{(i)}, v_r^{(i)}) \right)^{1/2},$$

and

$$\begin{aligned} s_i(v_r^{(i)}, v_r^{(i)}) &\leq H(\lambda_{l_{i+1}}^{(i)})^{-1} a_i(v_r^{(i)}, v_r^{(i)}) \leq H(\lambda_{l_{i+1}}^{(i)})^{-1} a_i(v^{(i)}, v^{(i)}) \\ &= H(\lambda_{l_{i+1}}^{(i)})^{-1} \int_{E_i} b |v^{(i)} \cdot t|^2 = H(\lambda_{l_{i+1}}^{(i)})^{-1} \int_{E_i} b |(u_{\text{snap}} - u_{\text{ms}}) \cdot t|^2. \end{aligned}$$

Hence,

$$\begin{aligned} \|u_{\text{snap}} - u_{\text{ms}}\|_{H(\text{curl})(a,b;D)}^2 &= -R(u_{\text{snap}} - u_{\text{ms}}) \\ &\leq \sqrt{H} \sum_{i=1}^{N_e} \|R_i\| (\lambda_{l_{i+1}}^{(i)})^{-1/2} \left(\int_{E_i} b |(u_{\text{snap}} - u_{\text{ms}}) \cdot t|^2 \right)^{1/2} \\ &\leq \sqrt{H} \left(\sum_{i=1}^{N_e} \|R_i\|^2 (\lambda_{l_{i+1}}^{(i)})^{-1} \right)^{1/2} \left(\sum_{i=1}^{N_e} \int_{E_i} b |(u_{\text{snap}} - u_{\text{ms}}) \cdot t|^2 \right)^{1/2} \\ &\leq \sqrt{\frac{C_V H}{h}} \left(\sum_{i=1}^{N_e} \|R_i\|^2 (\lambda_{l_{i+1}}^{(i)})^{-1} \right)^{1/2} \|u_{\text{snap}} - u_{\text{ms}}\|_{L^2(b;D)} \\ &\leq \sqrt{\frac{C_V H}{h}} \left(\sum_{i=1}^{N_e} \|R_i\|^2 (\lambda_{l_{i+1}}^{(i)})^{-1} \right)^{1/2} \|u_{\text{snap}} - u_{\text{ms}}\|_{H(\text{curl})(a,b;D)}. \end{aligned}$$

Therefore,

$$\|u_{\text{snap}} - u_{\text{ms}}\|_{H(\text{curl})(a,b;D)}^2 \leq \frac{C_V H}{h} \sum_{i=1}^{N_e} \|R_i\|^2 (\lambda_{l_{i+1}}^{(i)})^{-1}.$$

□

From the proof of Theorem 2, the error between the multiscale solution and the snapshot solution is bounded above by the norm of the global residual operator R , which in turn can be estimated by the sum of the error indicator $\|R_i\|^2 (\lambda_{l_{i+1}}^{(i)})^{-1}$.

Before we move on to the proof of the convergence of the offline adaptive method, we will prove the following lemma for the error indicator η_i .

Lemma 1. *For any $\alpha > 0$, we have*

$$(\eta_i^{m+1})^2 \leq (1 + \alpha) \frac{\lambda_{l_i^{m+1}}^{(i)}}{\lambda_{l_i^{m+1}+1}^{(i)}} (\eta_i^m)^2 + (1 + \alpha^{-1}) \left(\lambda_{l_i^{m+1}+1}^{(i)} \right)^{-1} \|u_{\text{ms}}^{m+1} - u_{\text{ms}}^m\|_{H(\text{curl})(a,b;\omega_i)}^2.$$

Proof. For any $v \in V_{\text{snap}}^{(i)}$, we have

$$R_i^m(v) = \int_{\omega_i} a (\nabla \times u_{\text{ms}}^m)(\nabla \times v) + b u_{\text{ms}}^m \cdot v - f \cdot v,$$

$$\text{and } R_i^{m+1}(v) = \int_{\omega_i} a (\nabla \times u_{\text{ms}}^{m+1})(\nabla \times v) + b u_{\text{ms}}^{m+1} \cdot v - f \cdot v.$$

Therefore

$$\begin{aligned} R_i^{m+1}(v) &= R_i^m(v) + \int_{\omega_i} a (\nabla \times (u_{\text{ms}}^{m+1} - u_{\text{ms}}^m)) (\nabla \times v) + b (u_{\text{ms}}^{m+1} - u_{\text{ms}}^m) \cdot v \\ &\leq R_i^m(v) + \|u_{\text{ms}}^{m+1} - u_{\text{ms}}^m\|_{H(\text{curl})(a,b;\omega_i)} \|v\|_{H(\text{curl})(a,b;\omega_i)}. \end{aligned}$$

Taking supremum with respect to v , we get

$$\eta_i^{m+1} \leq \left(\frac{\lambda_{l_i^{m+1}}^{(i)}}{\lambda_{l_i^{m+1}+1}^{(i)}} \right)^{1/2} \eta_i^m + \left(\lambda_{l_i^{m+1}+1}^{(i)} \right)^{-1/2} \|u_{\text{ms}}^{m+1} - u_{\text{ms}}^m\|_{H(\text{curl})(a,b;\omega_i)}.$$

Using the Young's inequality, we obtain the required result. \square

Using this lemma, we prove the following result for the convergence of the offline adaptive method.

Theorem 3. *There exists $\rho > 0$ and a non-increasing sequence of positive number $\{L_j\}$ such that*

$$\|u_{\text{snap}} - u_{\text{ms}}^{m+1}\|_{H(\text{curl})(a,b;D)} + \frac{1}{L_j} \sum_{i=1}^{N_e} (\eta_i^{m+1})^2 \leq \varepsilon_j \left(\|u_{\text{snap}} - u_{\text{ms}}^m\|_{H(\text{curl})(a,b;D)} + \frac{1}{L_j} \sum_{i=1}^{N_e} (\eta_i^m)^2 \right)$$

for any $j \leq m$, where ρ satisfies $1 - (1 - \delta_0)\theta < \rho < 1$, and $\varepsilon_j = \frac{C_{\text{err}} L_j + \rho}{C_{\text{err}} L_j + 1}$.

Proof. Let I be the set of indices i such that ω_i is chosen for basis enrichment. Using Lemma 1, we have

$$\sum_{i=1}^{N_e} (\eta_i^{m+1})^2 \leq \sum_{i=1}^{N_e} \left((1 + \alpha) \frac{\lambda_{l_i^{m+1}}^{(i)}}{\lambda_{l_i^{m+1}+1}^{(i)}} (\eta_i^m)^2 + (1 + \alpha^{-1}) \left(\lambda_{l_i^{m+1}+1}^{(i)} \right)^{-1} \|u_{\text{ms}}^{m+1} - u_{\text{ms}}^m\|_{H(\text{curl})(a,b;\omega_i)}^2 \right).$$

Writing the above sum as a sum over I and a sum over the complement of I , we have

$$\begin{aligned} \sum_{i=1}^{N_e} (\eta_i^{m+1})^2 &= \sum_{i \in I} (1 + \alpha) \frac{\lambda_{l_i^{m+1}}^{(i)}}{\lambda_{l_i^{m+1}+1}^{(i)}} (\eta_i^m)^2 + \sum_{i \notin I} (1 + \alpha) (\eta_i^m)^2 \\ &\quad + \sum_{i=1}^{N_e} (1 + \alpha^{-1}) \left(\lambda_{l_i^{m+1}+1}^{(i)} \right)^{-1} \|u_{\text{ms}}^{m+1} - u_{\text{ms}}^m\|_{H(\text{curl})(a,b;\omega_i)}^2 \end{aligned}$$

Using the criterion in the Step 4 in the offline adaptive algorithm, we have

$$\begin{aligned} \sum_{i=1}^{N_e} (\eta_i^{m+1})^2 &\leq \sum_{i \in I} (1 + \alpha) \delta_0 (\eta_i^m)^2 + \sum_{i \notin I} (1 + \alpha) (\eta_i^m)^2 \\ &\quad + \sum_{i=1}^{N_e} (1 + \alpha^{-1}) \left(\lambda_{l_i^{m+1}+1}^{(i)} \right)^{-1} \|u_{\text{ms}}^{m+1} - u_{\text{ms}}^m\|_{H(\text{curl})(a,b;\omega_i)}^2. \end{aligned}$$

Next, using the criterion in the Step 3 in the offline adaptive algorithm, we have

$$\begin{aligned}
\sum_{i=1}^{N_e} (\eta_i^{m+1})^2 &= (1 + \alpha) \sum_{i=1}^{N_e} (\eta_i^m)^2 - (1 + \alpha)(1 - \delta_0) \sum_{i \in I} (\eta_i^m)^2 \\
&\quad + \sum_{i=1}^{N_e} (1 + \alpha^{-1}) \left(\lambda_{l_i^{m+1}+1}^{(i)} \right)^{-1} \|u_{\text{ms}}^{m+1} - u_{\text{ms}}^m\|_{H(\text{curl})(a,b;\omega_i)}^2 \\
&= (1 + \alpha) \sum_{i=1}^{N_e} (\eta_i^m)^2 - (1 + \alpha)(1 - \delta_0)\theta \sum_{i=1}^{N_e} (\eta_i^m)^2 \\
&\quad + \sum_{i=1}^{N_e} (1 + \alpha^{-1}) \left(\lambda_{l_i^{m+1}+1}^{(i)} \right)^{-1} \|u_{\text{ms}}^{m+1} - u_{\text{ms}}^m\|_{H(\text{curl})(a,b;\omega_i)}^2 \\
&= (1 + \alpha)(1 - (1 - \delta_0)\theta) \sum_{i=1}^{N_e} (\eta_i^m)^2 \\
&\quad + \sum_{i=1}^{N_e} (1 + \alpha^{-1}) \left(\lambda_{l_i^{m+1}+1}^{(i)} \right)^{-1} \|u_{\text{ms}}^{m+1} - u_{\text{ms}}^m\|_{H(\text{curl})(a,b;\omega_i)}^2.
\end{aligned}$$

Since all ω_i 's will overlap for no more than 4 times, we have following estimate

$$\sum_{i=1}^{N_e} (1 + \alpha^{-1}) \left(\lambda_{l_i^{m+1}+1}^{(i)} \right)^{-1} \|u_{\text{ms}}^{m+1} - u_{\text{ms}}^m\|_{H(\text{curl})(a,b;\omega_i)}^2 \leq L_m \|u_{\text{ms}}^{m+1} - u_{\text{ms}}^m\|_{H(\text{curl})(a,b;D)}^2,$$

where

$$\begin{aligned}
L_m &= 4(1 + \alpha^{-1}) \left(\max_{1 \leq i \leq N_e} \left(\lambda_{l_i^{m+1}+1}^{(i)} \right)^{-1} \right) = 4(1 + \alpha^{-1})/\Lambda_*^m, \\
\Lambda_*^m &= \min_{1 \leq i \leq N_e} \lambda_{l_i^{m+1}+1}^{(i)}.
\end{aligned}$$

Note that L_m is non-increasing. Let $\rho = (1 + \alpha)(1 - (1 - \delta_0)\theta)$, and take α small enough such that $0 < \rho < 1$, we have the estimate

$$\begin{aligned}
\sum_{i=1}^{N_e} (\eta_i^{m+1})^2 &\leq \rho \sum_{i=1}^{N_e} (\eta_i^m)^2 + L_m \|u_{\text{ms}}^{m+1} - u_{\text{ms}}^m\|_{H(\text{curl})(a,b;D)}^2 \\
&\leq \rho \sum_{i=1}^{N_e} (\eta_i^m)^2 + L_j \|u_{\text{ms}}^{m+1} - u_{\text{ms}}^m\|_{H(\text{curl})(a,b;D)}^2.
\end{aligned} \tag{12}$$

On the other hand, combining (4) and (9), we have

$$\int_D a(\nabla \times (u_{\text{snap}} - u_{\text{ms}}^{m+1})) \cdot (\nabla \times v) + b(u_{\text{snap}} - u_{\text{ms}}^{m+1}) \cdot v = 0 \quad \forall v \in V_{\text{ms}}^{m+1}.$$

Taking $v = u_{\text{ms}}^{m+1} - u_{\text{ms}}^m \in V_{\text{ms}}^{m+1}$, we have

$$\int_D a(\nabla \times (u_{\text{snap}} - u_{\text{ms}}^{m+1})) \cdot (\nabla \times (u_{\text{ms}}^{m+1} - u_{\text{ms}}^m)) + b(u_{\text{snap}} - u_{\text{ms}}^{m+1}) \cdot (u_{\text{ms}}^{m+1} - u_{\text{ms}}^m) = 0.$$

Therefore,

$$\|u_{\text{snap}} - u_{\text{ms}}^m\|_{H(\text{curl})(a,b;D)}^2 = \|u_{\text{snap}} - u_{\text{ms}}^{m+1}\|_{H(\text{curl})(a,b;D)}^2 + \|u_{\text{ms}}^{m+1} - u_{\text{ms}}^m\|_{H(\text{curl})(a,b;D)}^2,$$

and consequently,

$$\|u_{\text{ms}}^{m+1} - u_{\text{ms}}^m\|_{H(\text{curl})(a,b;D)}^2 = \|u_{\text{snap}} - u_{\text{ms}}^m\|_{H(\text{curl})(a,b;D)}^2 - \|u_{\text{snap}} - u_{\text{ms}}^{m+1}\|_{H(\text{curl})(a,b;D)}^2.$$

Combining the above with (12), we obtain

$$\|u_{\text{snap}} - u_{\text{ms}}^{m+1}\|_{H(\text{curl})(a,b;D)}^2 + \frac{1}{L_j} \sum_{i=1}^{Ne} (\eta_i^{m+1})^2 \leq \|u_{\text{snap}} - u_{\text{ms}}^m\|_{H(\text{curl})(a,b;D)}^2 + \frac{\rho}{L_j} \sum_{i=1}^{Ne} (\eta_i^m)^2. \quad (13)$$

By Theorem 2, and for any $\beta > 0$, we have

$$\beta \|u_{\text{snap}} - u_{\text{ms}}^m\|_{H(\text{curl})(a,b;D)}^2 \leq \beta C_{\text{err}} \sum_{i=1}^{Ne} (\eta_i^m)^2. \quad (14)$$

Adding (13) and (14), we get

$$\|u_{\text{snap}} - u_{\text{ms}}^{m+1}\|_{H(\text{curl})(a,b;D)}^2 + \frac{1}{L_j} \sum_{i=1}^{Ne} (\eta_i^{m+1})^2 \leq (1-\beta) \|u_{\text{snap}} - u_{\text{ms}}^m\|_{H(\text{curl})(a,b;D)}^2 + (\beta C_{\text{err}} + \frac{\rho}{L_j}) \sum_{i=1}^{Ne} (\eta_i^m)^2.$$

Setting $\beta = \frac{1-\rho}{1+C_{\text{err}}L_j}$, we have

$$\|u_{\text{snap}} - u_{\text{ms}}^{m+1}\|_{H(\text{curl})(a,b;D)}^2 + \frac{1}{L_j} \sum_{i=1}^{Ne} (\eta_i^{m+1})^2 \leq (1-\beta) \|u_{\text{snap}} - u_{\text{ms}}^m\|_{H(\text{curl})(a,b;D)}^2 + \frac{1-\beta}{L_j} \sum_{i=1}^{Ne} (\eta_i^m)^2.$$

Finally, let $\varepsilon_j = 1 - \beta = \frac{C_{\text{err}}L_j + \rho}{C_{\text{err}}L_j + 1}$. Then we have completed the proof. \square

From Theorem 3, to have a fast convergence, we need ε_j to be small which requires a small ρ . Since $\rho = (1 + \alpha)(1 - (1 - \delta_0)\theta)$, we can take α small enough such that $\rho \approx (1 - (1 - \delta_0)\theta)$. So we need a small δ_0 and a large θ , which means that we need to select more ω_i 's to add basis; and for each selected ω_i , we add more eigenfunctions to offline basis. And this conclusion is coincide with our intuition.

Finally, we state and prove the convergence of the online adaptive method.

Theorem 4. *Let u_{ms}^m be the solution of the online adaptive method at the m -th iteration. Then we have*

$$\|u_{\text{snap}} - u_{\text{ms}}^{m+1}\|_{H(\text{curl})(a,b;D)}^2 \leq \|u_{\text{snap}} - u_{\text{ms}}^m\|_{H(\text{curl})(a,b;D)}^2 - \sum_{j=1}^{J^m} \|R_{\Omega_j^m}^m\|^2.$$

In addition, assume that the initial space contains l_i offline basis functions for the region ω_i . Then we have

$$\|u_{\text{snap}} - u_{\text{ms}}^{m+1}\|_{H(\text{curl})(a,b;D)}^2 \leq (1 - E) \|u_{\text{snap}} - u_{\text{ms}}^m\|_{H(\text{curl})(a,b;D)}^2$$

where

$$E = \sum_{j=1}^{J^m} \|R_{\Omega_j^m}^m\|^2 \left(C_{\text{err}} \sum_{i=1}^{Ne} \|R_i\|^2 (\lambda_{i+1}^{(i)})^{-1} \right)^{-1}.$$

Proof. For any $v \in V_{\text{ms}}^{m+1}$,

$$\begin{aligned}
& \left\| u_{\text{snap}} - u_{\text{ms}}^{m+1} + v \right\|_{H(\text{curl})(a,b;D)}^2 \\
&= \left\| u_{\text{snap}} - u_{\text{ms}}^{m+1} \right\|_{H(\text{curl})(a,b;D)}^2 + \left\| v \right\|_{H(\text{curl})(a,b;D)}^2 \\
&\quad + 2 \int_D a (\nabla \times (u_{\text{snap}} - u_{\text{ms}}^{m+1})) \cdot (\nabla \times v) + b (u_{\text{snap}} - u_{\text{ms}}^{m+1}) \cdot v \\
&= \left\| u_{\text{snap}} - u_{\text{ms}}^{m+1} \right\|_{H(\text{curl})(a,b;D)}^2 + \left\| v \right\|_{H(\text{curl})(a,b;D)}^2 \\
&\geq \left\| u_{\text{snap}} - u_{\text{ms}}^{m+1} \right\|_{H(\text{curl})(a,b;D)}^2.
\end{aligned}$$

Let $v = u_{\text{ms}}^{m+1} - u_{\text{ms}}^m + \phi_1^m + \dots + \phi_{J^m}^m \in V_{\text{ms}}^{m+1}$. Then we have

$$\begin{aligned}
& \left\| u_{\text{snap}} - u_{\text{ms}}^{m+1} \right\|_{H(\text{curl})(a,b;D)}^2 \\
&\leq \left\| u_{\text{snap}} - u_{\text{ms}}^m + \phi_1^m + \dots + \phi_{J^m}^m \right\|_{H(\text{curl})(a,b;D)}^2 \\
&= \left\| u_{\text{snap}} - u_{\text{ms}}^m \right\|_{H(\text{curl})(a,b;D)}^2 + \left\| \phi_1^m + \dots + \phi_{J^m}^m \right\|_{H(\text{curl})(a,b;D)}^2 \\
&\quad + 2 \int_D a (\nabla \times (u_{\text{snap}} - u_{\text{ms}}^m)) \cdot (\nabla \times (\phi_1^m + \dots + \phi_{J^m}^m)) + b (u_{\text{snap}} - u_{\text{ms}}^m) \cdot (\phi_1^m + \dots + \phi_{J^m}^m) \\
&= \left\| u_{\text{snap}} - u_{\text{ms}}^m \right\|_{H(\text{curl})(a,b;D)}^2 + \left\| \phi_1^m + \dots + \phi_{J^m}^m \right\|_{H(\text{curl})(a,b;D)}^2 \\
&\quad - 2 \int_D a (\nabla \times u_{\text{ms}}^m) \cdot (\nabla \times (\phi_1^m + \dots + \phi_{J^m}^m)) + b u_{\text{ms}}^m \cdot (\phi_1^m + \dots + \phi_{J^m}^m) - f \cdot (\phi_1^m + \dots + \phi_{J^m}^m).
\end{aligned}$$

Using the definition of the residual $R_{\Omega_j^m}^m$, we have

$$\begin{aligned}
& \left\| u_{\text{snap}} - u_{\text{ms}}^{m+1} + v \right\|_{H(\text{curl})(a,b;D)}^2 \\
&= \left\| u_{\text{snap}} - u_{\text{ms}}^m \right\|_{H(\text{curl})(a,b;D)}^2 + \sum_{j=1}^{J^m} \left\| \phi_j^m \right\|_{H(\text{curl})(a,b;D)}^2 - 2 \sum_{j=1}^{J^m} R_{\Omega_j^m}^m(\phi_j^m) \\
&= \left\| u_{\text{snap}} - u_{\text{ms}}^m \right\|_{H(\text{curl})(a,b;D)}^2 + \sum_{j=1}^{J^m} \left\| \phi_j^m \right\|_{H(\text{curl})(a,b;D)}^2 - 2 \sum_{j=1}^{J^m} \left\| \phi_j^m \right\|_{H(\text{curl})(a,b;D)}^2 \\
&= \left\| u_{\text{snap}} - u_{\text{ms}}^m \right\|_{H(\text{curl})(a,b;D)}^2 - \sum_{j=1}^{J^m} \left\| \phi_j^m \right\|_{H(\text{curl})(a,b;D)}^2 \\
&= \left\| u_{\text{snap}} - u_{\text{ms}}^m \right\|_{H(\text{curl})(a,b;D)}^2 - \sum_{j=1}^{J^m} \left\| R_{\Omega_j^m}^m \right\|^2.
\end{aligned}$$

This completes the proof of the first part. The proof for the second part is a direct consequence of Theorem 2. \square

We remark that, at each iteration, we need to choose proper Ω_j 's in order to obtain large value for the term $\sum_{j=1}^{J^m} \left\| R_{\Omega_j^m}^m \right\|^2$. Moreover, the convergence rate of the online adaptive method is $1 - E$. We remark that one obtains faster convergence if the initial space contains eigenfunctions corresponding to small eigenvalues.

5 Numerical Results

In this section, we will present two numerical examples with two different source fields $f = (f_1, f_2)$, shown in Figure 2, defined as follows:

$$\text{Example 1: } f_1 = \begin{cases} 100, & 0.1 < y < 0.2, \\ 10000, & 0.4 < y < 0.45, \\ 1, & \text{otherwise;} \end{cases} \quad f_2 = \begin{cases} -200, & 0.2 < x < 0.25, \\ 1500, & 0.65 < x < 0.75, \\ 5, & \text{otherwise.} \end{cases}$$

$$\text{Example 2: } f_1 = \begin{cases} 10, & x - y \leq -0.6, \\ -2, & x - y \geq 0.6, \\ 200, & x + y \leq 0.4, \\ 100, & x + y \geq 1.6, \\ 0, & \text{otherwise;} \end{cases} \quad f_2 = \begin{cases} 10, & x - y \leq -0.6, \\ -2, & x - y \geq 0.6, \\ -200, & x + y \leq 0.4, \\ -100, & x + y \geq 1.6, \\ 0, & \text{otherwise.} \end{cases}$$

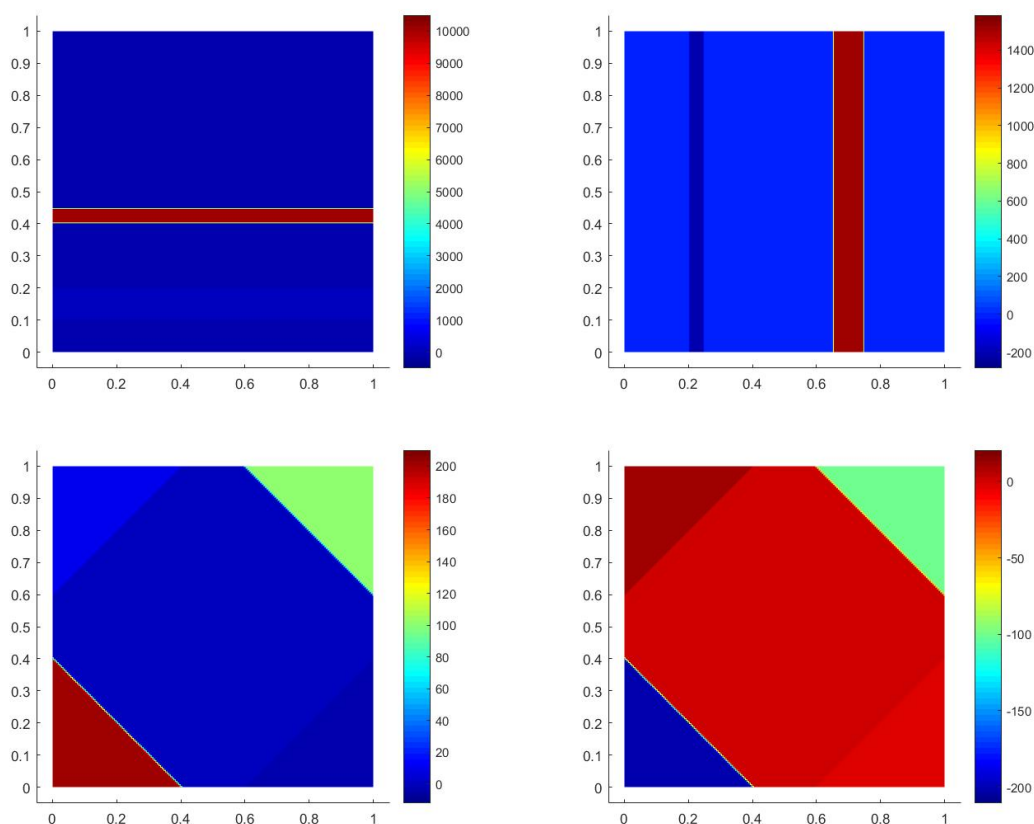


Figure 2: Top: f_1, f_2 in Example 1. Bottom: f_1, f_2 in Example 2.

In our simulations, we set $b = 1$. The space domain D is taken as the unit square $[0, 1] \times [0, 1]$ and is divided into 200×200 fine elements consisting of uniform squares. To measure the accuracy, we will use the following error quantities:

$$\tilde{e}_1 = \frac{\|u_h - u_{\text{snap}}\|_{H(\text{curl})(a,b;D)}}{\|u_h\|_{H(\text{curl})(a,b;D)}},$$

$$e_1 = \frac{\|u_{\text{snap}} - u_{\text{ms}}\|_{H(\text{curl})(a,b;D)}}{\|u_{\text{snap}}\|_{H(\text{curl})(a,b;D)}}, \quad e_2 = \frac{\|u_{\text{snap}} - u_{\text{ms}}\|_{L^2(D)}}{\|u_{\text{snap}}\|_{L^2(D)}}.$$

First of all, we consider the error of u_{snap} . We test different contrast values of a , i.e. $a = \kappa^2, \kappa^4, \kappa^6$, respectively, where κ is shown in Figure 3 with red denotes the value 10 and blue denotes the value 1. We also test different sizes of coarse blocks, i.e. $H = 0.1, 0.05, 0.025$. From Table 4, we can see that contrast values do not affect the error, and error converges in first order with respect to H . This verifies the conclusion in Theorem 1.

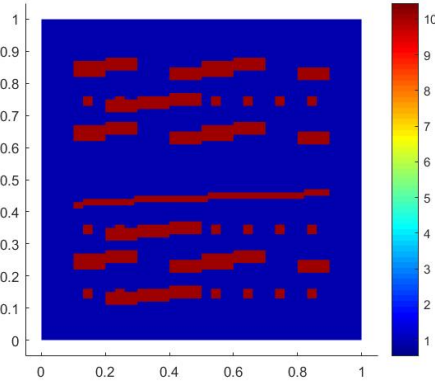


Figure 3: κ

$H \setminus$ Contrast	1e+2	1e+4	1e+6
0.1	22.02%	22.02%	22.02%
0.05	11.74%	11.71%	11.71%
0.025	5.73%	5.70%	5.70%

$H \setminus$ Contrast	1e+2	1e+4	1e+6
0.1	23.93%	23.92%	23.92%
0.05	11.90%	11.89%	11.89%
0.025	5.94%	5.94%	5.94%

Figure 4: \tilde{e}_1 comparison of different coarse size and different contrast values. Left: Example 1. Right: Example 2.

Next, we consider the error of u_{ms} using offline and online adaptive methods. We first compare offline adaptive method with uniform enrichment. Uniform enrichment means in each enrichment level we uniformly add one eigenfunction to multiscale space from each coarse neighborhood. We fix the contrast values to be 1e+4, and coarse block size $H = 0.1$. And we will keep the same setting for the future numerical analysis. For Example 1, we choose *initial number* = 1, $\theta=0.2$, $\delta_0=0.7$.

The error graph is shown in Figure 5. And for Example 2, we choose *initial number* = 2, $\theta=0.2$, $\delta_0=0.5$. The error graph is shown in Figure 6. We can see the error decays faster while using offline adaptive method than using uniform enrichment.

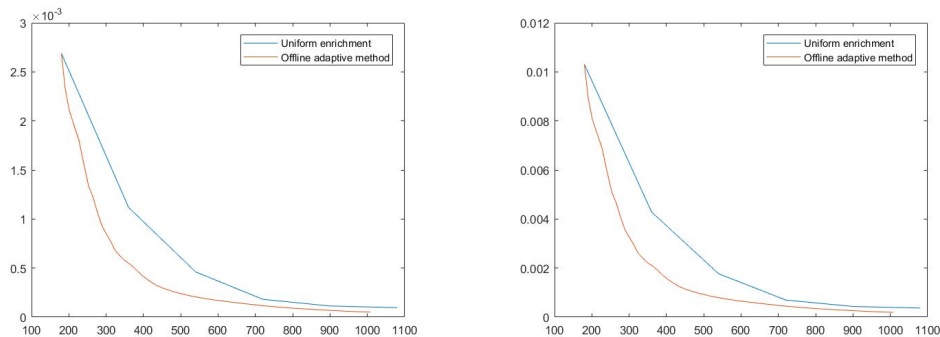


Figure 5: Error comparison for Example 1. Along x-axis: Dimensions of V_{ms} (DOF). Along y-axis: Relative errors. Left: e_1 . Right: e_2 .

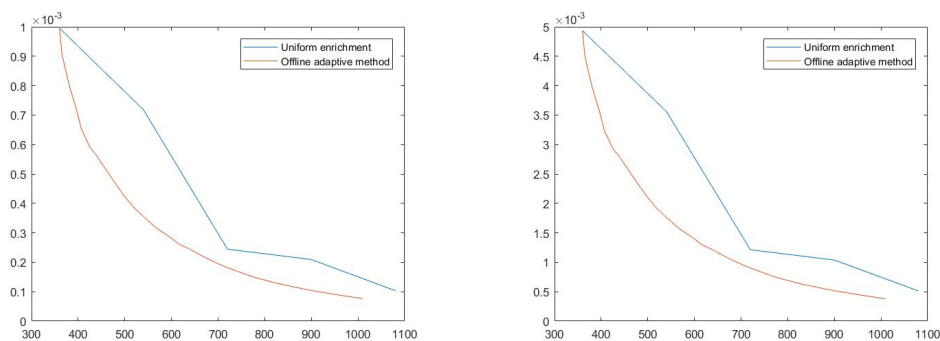


Figure 6: Error comparison for Example 2. Along x-axis: Dimensions of V_{ms} (DOF). Along y-axis: Relative errors. Left: e_1 . Right: e_2 .

Next, we introduce a new algorithm which combines offline adaptive method and online adaptive method. The idea is that we first use offline adaptive method, and want to switch to online adaptive method when error decay becomes low. To achieve this, we use a user-defined criterion and the full algorithm is shown in **Algorithm 1**.

For both examples, we keep the same setting of *initial number*, θ and δ_0 as before. And we choose $\delta = 0.5$, *total online iterations* = 4 and *percentage* = 25%. Then the error graphs are shown in Figures 7 and 8. We can see the point very clear when we switch to online adaptive method, and the error decay becomes much faster after that.

We give a final note regarding the implementation. In the part of online adaptive method, we will select non-overlapping regions. Here we introduce one option used in the numerical test above. We define a term "square coarse region", which represents a region consisting of 2×2 coarse

Algorithm 1 Offline-online adaptive method

Choose *total online iterations*, *initial number*, $0 < \theta, \delta_0$, *percentage* < 1 .

Set $flag = 0$, $m = 0$, $J = \emptyset$.

while $flag = 0$ **do** ▷ During the While loop, we use offline method.

if $m = 0$ **then**

 In each ω_i , set $l_i = \textit{initial number}$ and take first l_i eigenfunctions as multiscale basis.

else

 For each ω_i , we compute the local error indicators η_i . And we find the smallest k , such that: if we define a subset I of $\{\omega_i\}_1^{N_e}$ and the members in I are just corresponding to the k largest η_i , the following condition holds

$$\sum_{\omega_i \in I} \eta_i^2 \geq \theta \sum_{i=1}^{N_e} \eta_i^2.$$

for all $\omega_i \in I$ **do**

 Take the smallest s_i such that

$$\frac{\lambda_{l_i+1}^{(i)}}{\lambda_{l_i+s_i+1}^{(i)}} \leq \delta_0.$$

 Add s_i more eigenfunctions to multiscale basis.

if $\frac{\lambda_{l_i+s_i}^{(i)}}{\lambda_{l_i+s_i+1}^{(i)}} \geq \delta$ **then**

 Add ω_i to J . ▷ J collects the coarse neighborhoods that reach the bound.

end if

if $\frac{|J|}{|\{\omega_i\}_1^{N_e}|} \geq \textit{percentage}$ **then** ▷ $|\cdot|$ represents the cardinality of a set.

$flag = 1$. ▷ There are enough coarse neighborhoods reaching the bound.

end if

end for

$l_i \leftarrow l_i + s_i$.

end if

 Compute multiscale solution.

$m \leftarrow m + 1$.

end while

$m = 1$.

while $m \leq \textit{total online iterations}$ **do** ▷ During the While loop, we use online method.

 Select non-overlapping regions, and add online basis function to multiscale basis.

 Compute multiscale solution.

$m \leftarrow m + 1$.

end while

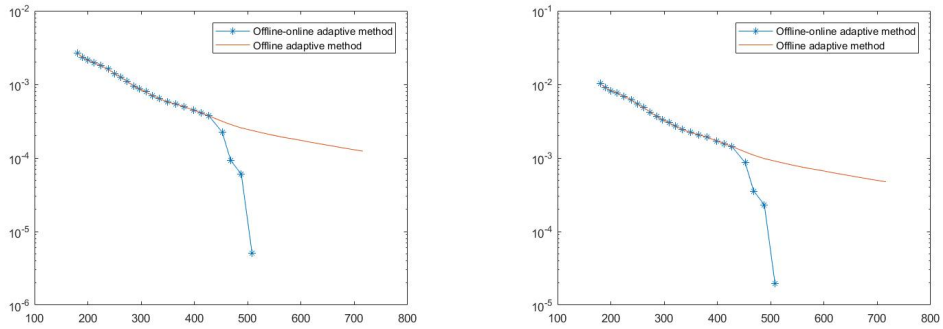


Figure 7: Error comparison for Example 1. Along x-axis: Dimensions of V_{ms} (DOF). Along y-axis: Relative errors. Left: e_1 . Right: e_2 .

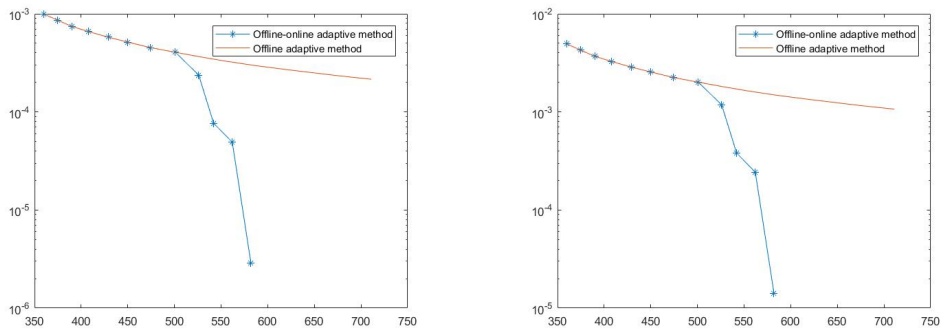


Figure 8: Error comparison for Example 2. Along x-axis: Dimensions of V_{ms} (DOF). Along y-axis: Relative errors. Left: e_1 . Right: e_2 .

elements. Square coarse regions are denoted by $\omega_{i,j}$, where $i = 1, \dots, N_x - 2$ and $j = 1, \dots, N_y - 2$ and N_x and N_y are the number of coarse nodes in the x and y directions respectively. We will divide all $\omega_{i,j}$ into four group I_1, I_2, I_3 , and I_4 depending on the party of (i, j) . Then each group is a set of non-overlapping regions. At each level, in order to determine which group we choose, we need to compare $\sum_{\omega_{i,j} \in I_1} \|R_{\omega_{i,j}}^m\|^2$, $\sum_{\omega_{i,j} \in I_2} \|R_{\omega_{i,j}}^m\|^2$, $\sum_{\omega_{i,j} \in I_3} \|R_{\omega_{i,j}}^m\|^2$ and $\sum_{\omega_{i,j} \in I_4} \|R_{\omega_{i,j}}^m\|^2$, and choose the largest one.

6 Conclusion

In this paper, we present an adaptive multiscale method for H(curl)-elliptic problems with heterogeneous coefficients. We develop an adaptive basis enrichment procedure for the selection of basis functions. We also propose an offline-online approach, so that one can automatically use both offline and online basis functions. In addition, the convergence of both the offline and the online adaptive methods are shown, and our results indicate that the convergence is independent of the

heterogeneities and the contrast of the coefficients. Finally, some numerical results are presented to validate the scheme. In the future, we plan to develop multiscale method using the constraint energy minimization approach [11, 6], as well as a unified approach based on the idea in this paper and the constraint energy minimization approach.

References

- [1] J. E. Aarnes. On the use of a mixed multiscale finite element method for greater flexibility and increased speed or improved accuracy in reservoir simulation. SIAM J. Multiscale Modeling and Simulation, 2:421–439, 2004.
- [2] Todd Arbogast. Analysis of a two-scale, locally conservative subgrid upscaling for elliptic problems. SIAM Journal on Numerical Analysis, 42(2):576–598, 2004.
- [3] C-C Chu, Ivan Graham, and T-Y Hou. A new multiscale finite element method for high-contrast elliptic interface problems. Mathematics of Computation, 79(272):1915–1955, 2010.
- [4] E Chung and Wing Tat Leung. A sub-grid structure enhanced discontinuous Galerkin method for multiscale diffusion and convection-diffusion problems. Comput. Phys, 14:370–392, 2013.
- [5] Eric Chung, Yalchin Efendiev, and Thomas Y Hou. Adaptive multiscale model reduction with generalized multiscale finite element methods. Journal of Computational Physics, 320:69–95, 2016.
- [6] Eric Chung, Yalchin Efendiev, and Wing Tat Leung. Constraint energy minimizing generalized multiscale finite element method in the mixed formulation. arXiv preprint arXiv:1705.05959, 2017.
- [7] Eric T Chung, Yalchin Efendiev, and Wing Tat Leung. An adaptive generalized multiscale discontinuous Galerkin method (GMsDGM) for high-contrast flow problems. 2014. arXiv preprint arXiv:1409.3474.
- [8] Eric T Chung, Yalchin Efendiev, and Wing Tat Leung. Generalized multiscale finite element methods for wave propagation in heterogeneous media. Multiscale Modeling & Simulation, 12(4):1691–1721, 2014.
- [9] Eric T Chung, Yalchin Efendiev, and Wing Tat Leung. An online generalized multiscale discontinuous galerkin method (gmsdgm) for flows in heterogeneous media. arXiv preprint arXiv:1504.04417, 2015.
- [10] Eric T Chung, Yalchin Efendiev, and Wing Tat Leung. Residual-driven online generalized multiscale finite element methods. arXiv preprint arXiv:1501.04565, 2015.
- [11] Eric T Chung, Yalchin Efendiev, and Wing Tat Leung. Fast online generalized multiscale finite element method using constraint energy minimization. Journal of Computational Physics, 355:450–463, 2018.
- [12] Eric T Chung, Yalchin Efendiev, and Guanglian Li. An adaptive GMsFEM for high-contrast flow problems. Journal of Computational Physics, 273:54–76, 2014.

- [13] E.T. Chung, Y. Efendiev, and S. Fu. Generalized multiscale finite element method for elasticity equations. International Journal on Geomathematics, 5:225–254, 2014.
- [14] Louis J Durlofsky. Numerical calculation of equivalent grid block permeability tensors for heterogeneous porous media. Water resources research, 27(5):699–708, 1991.
- [15] Yalchin Efendiev, Juan Galvis, and Thomas Y Hou. Generalized multiscale finite element methods (GMsFEM). Journal of Computational Physics, 251:116–135, 2013.
- [16] Yalchin Efendiev, Juan Galvis, and Xiao-Hui Wu. Multiscale finite element methods for high-contrast problems using local spectral basis functions. Journal of Computational Physics, 230(4):937–955, 2011.
- [17] Yalchin Efendiev and Thomas Y Hou. Multiscale finite element methods: theory and applications, volume 4. Springer Science & Business Media, 2009.
- [18] Yalchin Efendiev, Thomas Y Hou, Victor Ginting, et al. Multiscale finite element methods for nonlinear problems and their applications. Communications in Mathematical Sciences, 2(4):553–589, 2004.
- [19] Björn Engquist and Olof Runborg. Heterogeneous multiscale methods. Communications in Mathematical Science, 1(1):132, 2013.
- [20] K. Gao, E.T. Chung, R. Gibson, S. Fu, and Y. Efendiev. A numerical homogenization method for heterogenous, anisotropic elastic media based on multiscale theory. Geophysics, 80:D385–D401, 2015.
- [21] K. Gao, S. Fu, R. Gibson, E.T. Chung, and Y. Efendiev. Generalized multiscale finite element method (GMsFEM) for elastic wave propagation in heterogeneous, anisotropic media. J. Comput. Phys., 295:161–188, 2015.
- [22] Mehdi Ghommam, Michael Presho, Victor M Calo, and Yalchin Efendiev. Mode decomposition methods for flows in high-contrast porous media. global–local approach. Journal of Computational Physics, 253:226–238, 2013.
- [23] R. Gibson, K. Gao, E. Chung, and Y. Efendiev. Multiscale modeling of acoustic wave propagation in two-dimensional media. Geophysics, 79:T61–T75, 2014.
- [24] Patrick Henning, Mario Ohlberger, and Barbara Verfürth. A new heterogeneous multiscale method for time-harmonic Maxwell’s equations. SIAM Journal on Numerical Analysis, 54(6):3493–3522, 2016.
- [25] Thomas Y Hou and Xiao-Hui Wu. A multiscale finite element method for elliptic problems in composite materials and porous media. Journal of computational physics, 134(1):169–189, 1997.
- [26] P. Jenny, S. H. Lee, and H. Tchelepi. Multi-scale finite volume method for elliptic problems in subsurface flow simulation. J. Comput. Phys., 187:47–67, 2003.
- [27] Peter Monk. Finite element methods for Maxwell’s equations. Oxford University Press, 2003.

- [28] Jean-Claude Nédélec. Mixed finite elements in R³. Numerische Mathematik, 35(3):315–341, 1980.
- [29] Xiao-Hui Wu, Y Efendiev, and Thomas Y Hou. Analysis of upscaling absolute permeability. Discrete and Continuous Dynamical Systems Series B, 2(2):185–204, 2002.